

Can a passive hopper hop forever?

C. K. Reddy and R. Pratap*

Department of Mechanical Engineering, Indian Institute of Science, Bangalore 560 012, India

It is now understood that stable gait can be exhibited by passive walking models. The energy losses associated with collisions in such passive models play a central role in achieving stable gait. We study a simple passive model for hopping. The model consists of a two-mass, one-spring system. The only mode of energy dissipation is through the plastic collisions with the rigid ground. We show that there exist solutions that involve lossless inelastic collisions and thus lead to incessant hopping. The global dynamics of the hopping model is studied by constructing a one-dimensional map. We show that the fixed points of the one-dimensional map exhibit one-way stability. The consequences of an infinite number of fixed points and their one-way stability on the dynamics is also studied and it is shown that there exists a nested basin of attraction for each fixed point of the system, making the fate of an individual orbit unpredictable.

THE relentless search for complex and chaotic motions over the last three decades has led to fascinating progress in the dynamical systems theory. It is almost an established fact that a nonlinear system, deterministic or stochastic, is capable of exhibiting chaotic response if forced appropriately. The key to the complexity in response is the nonlinearity of the system. How nonlinear does a system have to be to exhibit chaotic motion? This question has been asked over and over in the past. While no definitive measures have been devised to answer ‘how nonlinear’, there have been several successful attempts at creating models with simple nonlinear terms that show a complex response of such models (e.g. Lorenz equation, Duffing oscillator, etc¹.)

One class of such simple systems that exhibit complex response but possess seemingly simple nonlinearity is impacting systems. Impacting systems have special significance from two different points of view: (i) they are prevalent in engineering applications²⁻⁵, (ii) they usually represent non-smooth dynamical systems that need special care in analysis⁶⁻⁸.

Among mechanical systems that involve impacts or collisions, there is a class of systems that represents gait and locomotion. Although the robotics community has been actively studying gait mechanics for a long time^{9,10}, there has been a renewed interest in this field, from a somewhat different perspective, ever since the pioneering

work of Ted McGeer¹¹. He showed that it is possible to build a passive (i.e. no controls, no external source of driving) legged walker that has stable gait on gentle slopes. Since then, there have been numerous studies¹²⁻¹⁴ on passive walkers. In passive robots, the impacts with the ground assume central significance as the sole energy dissipating mechanism. Naturally, impacts in such systems play a crucial role in the stability of motion.

In this paper, we present a particularly simple impacting system – a hopper – that has one-dimensional linear motion for most part, and intermittent inelastic impacts with the ground. We call this hopper ‘the Chatterjee Chatterer’, named after Anindya Chatterjee¹⁵ who first suggested this model. This hopper is intended at modelling the dynamics of passive hopping. The goal is to study the dynamics and energetics of hopping in order to gain a better understanding of such motions in animal locomotion. The model of the hopper is described in the next section. The only source of nonlinearity in the system is from the impacts, which introduces discontinuity in the otherwise linear behaviour of the system. The impacts are also the only source of energy dissipation. The subsequent analysis of the motion of the hopper is guided by the quest for finding solutions that correspond to incessant hopping despite the collisions with the ground. The solutions found have a peculiar characteristic of one-way stability, a phenomenon not observed in mechanical systems so far, to the best of our knowledge. Furthermore, these motions have nested basins of attraction that show self-similar structure at finer scales. Thus, the hopper exhibits incredibly complex response even under the simplest possible conditions of passive hopping.

Mechanical model for hopping

The model used to study hopping in this paper is a passive one-dimensional mechanical model. The study of such a passive model is motivated by the fact that gait can be generated and sustained without any external control¹¹. The one-dimensional simplified hopping model is shown in Figure 1. The model consists of two concentrated masses and a massless, linear spring. The impacts of the lower mass with the rigid ground are perfectly plastic. The plastic impact implies that the velocity of the lower mass becomes zero when it strikes the ground. All energy dissipating processes, other than the plastic collisions are neglected. The forces acting on both the masses are shown in

*For correspondence. (e-mail: pratap@mecheng.iisc.ernet.in)

Figure 1. The equations of motion during flight for each mass can be easily derived from the free body diagram (shown in Figure 1) and the linear momentum balance. The equations are:

$$m_1 \ddot{x}_1 = -k(x_1 - x_2) - m_1 g, \tag{1}$$

$$m_2 \ddot{x}_2 = k(x_1 - x_2) - m_2 g, \tag{2}$$

where m_1 is the upper mass, m_2 is the lower mass, x_1 is the displacement of the upper mass and x_2 is the displacement of the lower mass. The displacements of the two masses can be normalized with respect to $x_0 = m_2 g / k$, the displacement of the spring required to balance gravity for the lower mass, and the equations of motion can be rewritten in terms of non-dimensional variables involving a single system parameter $M = m_2 / m_1$ as follows:

$$\ddot{y}_1 = -M(y_1 - y_2) - 1, \tag{3}$$

$$\ddot{y}_2 = (y_1 - y_2) - 1, \tag{4}$$

where $y_1 = x_1 / x_0$ is the non-dimensional displacement of the upper mass and $y_2 = x_2 / x_0$ is the non-dimensional displacement of the lower mass. The derivatives are with respect to non-dimensional time $t = \mathbf{w}t$, where $\mathbf{w} = \sqrt{k/m_2}$.

Conditions for lossless collisions

The inelastic impacts of the lower mass with the ground are the only form of dissipation in the model. Hence if the velocity of the lower mass is zero at the instant it touches the ground then there will not be any loss of energy. Let the initial conditions be such that the lower mass is just about to lift after a period of steady contact with the ground, i.e.

$$y_2(0) = \dot{y}_2(0) = 0,$$

$$y_1(0) = 1,$$

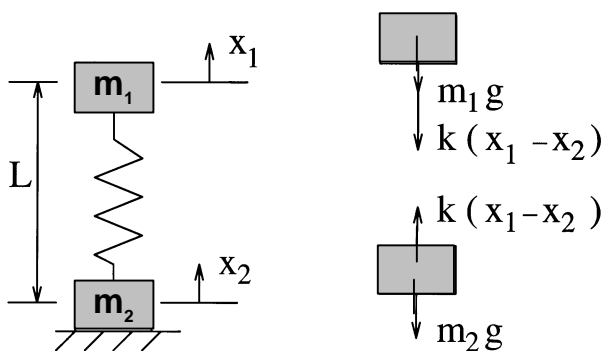


Figure 1. (Left) Model for hopping. The model consists of two concentrated masses and a massless linear spring. (Right) Free body diagram of the system in flight. L is the free length of the spring.

$$\dot{y}_1(0) = \mathbf{a},$$

where \mathbf{a} is the non-dimensional initial velocity of the upper mass at take-off. When the hopper lands (i.e. lower mass strikes the ground), we require that $\dot{y}_2 = 0$ in order to have lossless collisions. We further require that $\ddot{y}_2 = 0$ at the instant of collision, so that the successive hops are lossless and we get periodic, energy conserving motion¹⁶. Our goal is to find all the initial velocities, \mathbf{a} , of the upper mass that give rise to the above condition for lossless collisions. From eqs (3) and (4) we see that this is an inverse initial value problem. Equations (3) and (4) are simple second-order, linear differential equations that admit harmonic solutions with respect to the centre of mass. Since the conditions at impact are specified, the solution to our inverse initial value problem requires solution of transcendental equations (solutions of eqs (3) and (4)). Carrying out the necessary algebra, we find the following condition on \mathbf{a} that satisfies the prescribed impact conditions:

$$\mathbf{a} = \tan \mathbf{a}. \tag{5}$$

The solutions of eq. (5) give the initial velocities of the upper mass at take-off that give lossless collisions. It can be noted that there are infinite solutions that give incessant hopping. Also, the \mathbf{a} 's which lead to incessant hopping are independent of the mass ratio M . The values of the first three solutions are $\mathbf{a} = 4.493409458, 7.725251837, 10.9041216$. In the subsequent discussion, we refer to these values of \mathbf{a} by $\mathbf{a}^{*1}, \mathbf{a}^{*2}, \mathbf{a}^{*3}$, etc.

One-dimensional maps

Dynamical systems which are discrete in time are represented by difference equations or maps¹⁷. A map is expressed in the general form $\mathbf{x}_{n+1} = \mathbf{f}(\mathbf{x}_n)$, where \mathbf{x}_n is in general an n -dimensional vector. The function \mathbf{f} takes values, say \mathbf{x}_n , from the n -dimensional space and gives back \mathbf{x}_{n+1} . A map is called a one-dimensional map when x_n is a scalar. If one starts with an initial x_0 , then $f(x_0)$ gives x_1 , $f(x_1)$ gives x_2 and so on. This recursive operation is schematically shown in Figure 2. The sequence $\{x_0, x_1, x_2, \dots\}$ is called the orbit of x_0 . A point x^* is called a fixed point of the map, if $f(x^*) = x^*$. This means that the orbit starting at x^* remains at x^* for all future iterations. The reader, if unfamiliar with maps, should refer to any

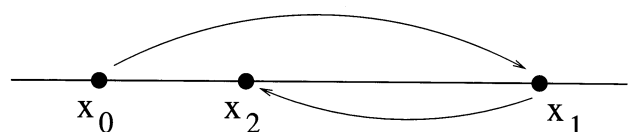


Figure 2. Iterates of a one-dimensional map with the starting value being x_0 .

elementary book on dynamical systems^{1,18}. We now briefly discuss the mechanism of finding orbits of a point in one-dimensional maps (we need it in the next section to understand the dynamics of the hopper). A generic one-dimensional map $x_{n+1} = f(x_n)$, is shown schematically in Figure 3. Given the initial condition x_0 , we draw a vertical line until it intersects the graph of f . The ordinate of the intersection point is x_1 . To get x_2 from x_1 , we trace a horizontal line till it intersects the identity map, $x_{n+1} = x_n$, and then move vertically to the curve again to get x_2 . The process is repeated to get the orbit of x_0 . The function f need not be an explicit function.

One-dimensional map for the hopping model

We can construct a one-dimensional map for the hopping model in the following manner. The different phases during a hop are shown in Figure 4. We are interested in finding the value of \mathbf{a} at the next gradual take-off, given the initial value of \mathbf{a} . Let \mathbf{a}_n be the non-dimensional velocity of the upper mass when the lower mass is about to move at the n th hop. The ‘about to move’ condition implies that $y_1 = 1$ at take-off. The system takes off and then lands again. The lower mass impacts the ground with non-zero velocity and loses all its kinetic energy in the plastic collision. After the impact, depending upon the value of y_1 , the hopper can have a sudden hop or a gradual hop. If $y_1 > 1$, then the hopper has a sudden hop. Otherwise, the lower mass rests on the ground while the upper mass moves till y_1 becomes equal to unity again, when the hopper takes the next gradual hop. Let \mathbf{a}_{n+1} be the non-dimensional velocity of the upper mass at the next gradual hop, i.e. $(n + 1)$ th hop. We seek a mapping function G , which maps \mathbf{a}_n to \mathbf{a}_{n+1} . Hence the one-dimensional map can be written as,

$$\mathbf{a}_{n+1} = G(\mathbf{a}_n). \tag{6}$$

The function G is not known explicitly. Given an initial \mathbf{a}_0 , let us look at the steps involved in calculating \mathbf{a} at the

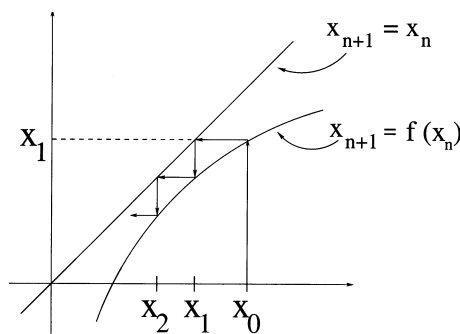


Figure 3. Staircase construction to get the iterates of a one-dimensional map.

next gradual take-off, i.e. \mathbf{a}_1 . The initial conditions at take-off are:

$$\begin{aligned} y_1(0) &= y_{10} = 1, \\ \dot{y}_1(0) &= \dot{y}_{10} = \mathbf{a}_0, \\ y_2(0) &= y_{20} = 0, \\ \dot{y}_2(0) &= \dot{y}_{20} = 0. \end{aligned}$$

The time of flight (the time taken before the lower mass lands) is obtained by solving a transcendental equation, which then gives the conditions just before impact. Since the collision is plastic, the lower mass loses all its kinetic energy, i.e. the velocity of the lower mass becomes zero. The velocity and the displacement of the upper mass remain unchanged. Thus, the conditions immediately after impact are determined. If the non-dimensional displacement of the upper mass immediately after impact is greater than 1, the system takes off as soon as it lands with the conditions immediately after landing being the initial conditions. Otherwise, the lower mass rests on the ground while the upper mass moves till the non-dimensional displacement of the upper mass becomes equal to 1, where we have a gradual take-off again. As the energy of the system is conserved during the contact phase, an energy balance gives the conditions at the next gradual take-off. Let \mathbf{a}_1 be the velocity of the upper mass at the next gradual take-off. Now, \mathbf{a}_1 is the initial condition. The above sequence of steps is repeated to obtain \mathbf{a}_2 and so on. The sequence $\{\mathbf{a}_0, \mathbf{a}_1, \mathbf{a}_2, \dots\}$ is the orbit of \mathbf{a}_0 . This is shown schematically in Figure 5 a. For example, if we start with $\mathbf{a}_0 = 10$, then the table in Figure 5 b shows the iterates of the map for $M = 0.15$. The velocity \mathbf{a} of the upper mass characterizes the total energy at take-off for a given M . Every impact is associated with a loss of energy and hence every iterate of the map is associated with a decrease in the value of \mathbf{a} . Hence, the one-dimensional map can exist only below the line of unit slope. At the fixed points of the map, we have $\mathbf{a}_n = \mathbf{a}_{n+1}$. The fixed points are the solutions of the equation $\mathbf{a} = \tan \mathbf{a}$. We take a range of values of initial \mathbf{a} 's and calculate the corresponding \mathbf{a} 's at the next gradual take-off. We plot the values of \mathbf{a} at the next take-off on the y -axis and the corresponding initial \mathbf{a} 's on the x -axis to get

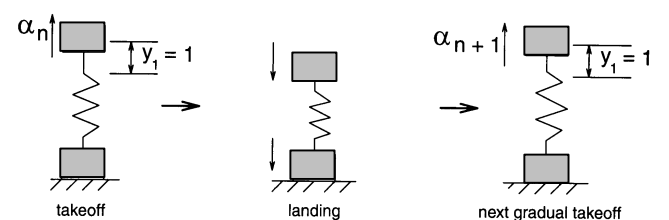


Figure 4. Different phases during a hop.

the one-dimensional map. The one-dimensional map thus obtained is shown in Figure 6. The one-dimensional map has several breaks. These breaks correspond to the initial \mathbf{a} 's for which there is no second hop, i.e. there is no second iterate. For such initial \mathbf{a} 's, the energy carried by the upper mass is not sufficient to lift the lower mass. So, the lower mass rests on the ground and the upper mass performs oscillations.

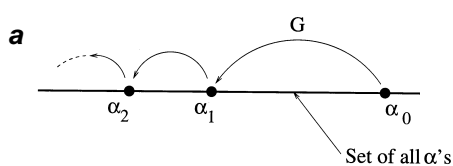
Stability of the fixed points in the hopping model

In a dynamical system, one of the most important features is a fixed point. Typically, the first step in the analysis of any dynamical system is the determination of the fixed points and the analysis of their stability. A fixed point is stable if the orbit starting from a nearby point converges to the fixed point and unstable if the orbit diverges. Now, we discuss the stability of the fixed points in the hopping model. More precisely, we study the fate of the orbit of an initial condition close to the fixed point. Since our map G is not explicit, we numerically plot the map very close to one of the fixed points. The map G around a fixed point is shown in Figure 7. From the staircase construction shown in the figure, we see that for initial conditions close to the fixed point on the right side, the orbits converge to the fixed point. But for initial conditions on the left side of the fixed point, the orbits diverge. Thus, the fixed point is stable from one-side. This is intuitive because \mathbf{a} is a measure of the energy of the system and every iterate of the map is associated with a decrease in the value of \mathbf{a} . Hence the fixed point can be stable only from the right side. This one-way stability is not a generic case. In fact, it is normally dismissed as a pathological case in the

mathematical theory of dynamical systems. To the best of our knowledge, this is the first example of a mechanical system that exhibits such stability.

Effect of system parameters on the map of the hopping model

The interval of attraction is the interval around the fixed point such that the orbit of any initial point in the interval converges to the fixed point. The mass ratio M is the only non-dimensional system parameter, apart from \mathbf{a} , which affects the dynamics of the hopper. Since M is the ratio of m_2 to m_1 , a lower value of M would mean a lower energy associated with the lower mass, which in turn implies a lower loss of energy after each impact. A lower loss of energy after an impact would essentially lead to a larger attracting region around the fixed point. This is evident from Figure 8 *a*. It is clear that the attracting interval around the fixed point \mathbf{a}^{*1} increases as M is decreased.



b

α_n	α_{n+1}
10	7.980369
7.980369	7.522029
7.522029	6.796374
6.796374	5.460504
5.460504	4.155416

Figure 5. *a*, One-dimensional map G for the hopping model; *b*, Iterates of the map with an initial value $\mathbf{a}_0 = 10$ and $M = 0.15$.

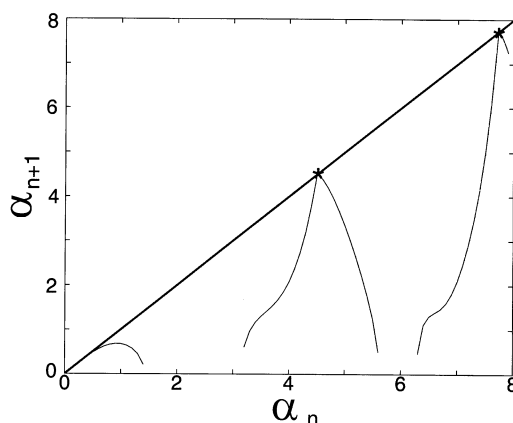


Figure 6. One-dimensional map for the hopping model with $M = 1$. Fixed points of the map are marked by “*”.

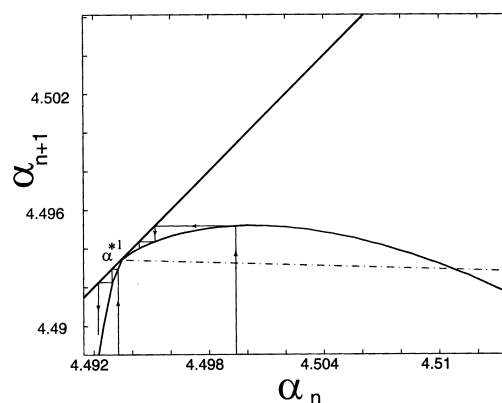


Figure 7. One-dimensional map for the hopping model around $\mathbf{a}^{*1} = 4.4934$ with $M = 1$. The interval of attraction is from $\mathbf{a} = 4.4934$ to $\mathbf{a} = 4.509$.

Figure 8 *b* shows how the map varies between two successive fixed points as M is varied. Higher the value of M , higher the energy lost at impact and lower the value of \mathbf{a} at the next gradual take-off. At higher values of M , we get a discontinuous map because the energy dissipated at the first impact is so large that the remaining energy is not sufficient for the next take-off.

Basin of attraction for the hopping model

As mentioned in the previous section, the fixed points have one-way stability. Each fixed point has an interval of attraction around it. Now, the *basin of attraction* of a fixed point is defined as the set of all points whose orbits go to that fixed point for some n including $n \rightarrow \infty$. We have already identified a set of points (the interval of attraction on the right side of the fixed points) that satisfy this criterion. We now show that there are several other sets, actually a countable infinity, of such points that form the basin of attraction of the fixed points. Let us consider

the schematic map as shown in Figure 9 *a*. The interval A is the interval of attraction for the fixed point \mathbf{a}^{*1} . To see whether there exist other intervals such that the orbits of any point in these intervals converge to \mathbf{a}^{*1} , we can use the staircase construction in the reverse. It can be easily seen that orbits from any initial \mathbf{a} lying in the intervals $A1, A2, A21, A22$, etc., converge to the fixed point \mathbf{a}^{*1} . The union of all such intervals for a given M forms the basin of attraction for the fixed point \mathbf{a}^{*1} . But there exist infinite such fixed points and each has its own basin of attraction. This is clear from the map shown in Figure 9 *b*. The dashed lines show the orbit of the points converging to the first fixed point $\mathbf{a}^{*1} = 4.4934$, the solid lines show the orbit of the points converging to the second fixed point $\mathbf{a}^{*2} = 7.7252$, and so on. The basins of attraction of different fixed points are thus nested. This is shown in Figure 10. We follow a colour scheme; we plot all points which lead to the first fixed point \mathbf{a}^{*1} with green, the points which lead to the second fixed point \mathbf{a}^{*2} with red, the points leading to the third fixed point with blue and so on.

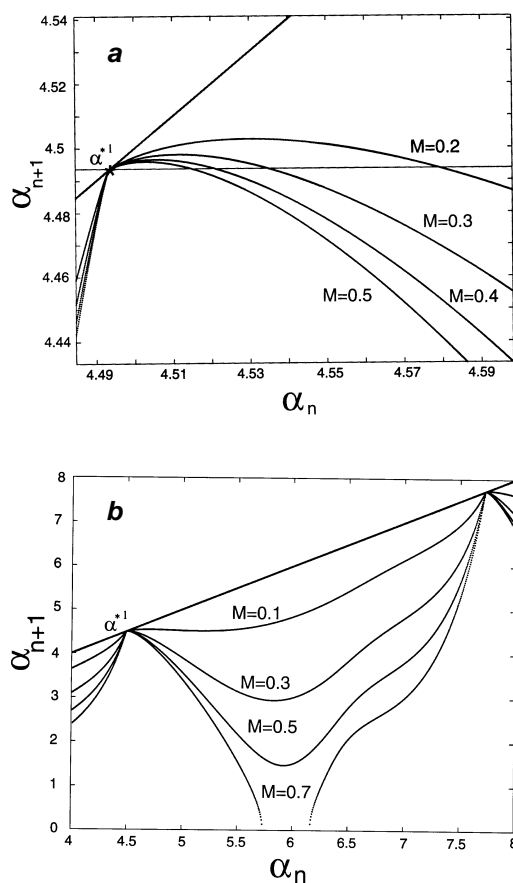


Figure 8. *a*, Variation of the interval of attraction with increasing values of M around the fixed point $\mathbf{a}^{*1} = 4.4934$. The interval of attraction shrinks with increasing values of M ; *b*, One-dimensional map for the hopping model between successive fixed points $\mathbf{a}^{*1} = 4.4934$ and $\mathbf{a}^{*2} = 7.7252$ for different values of M .

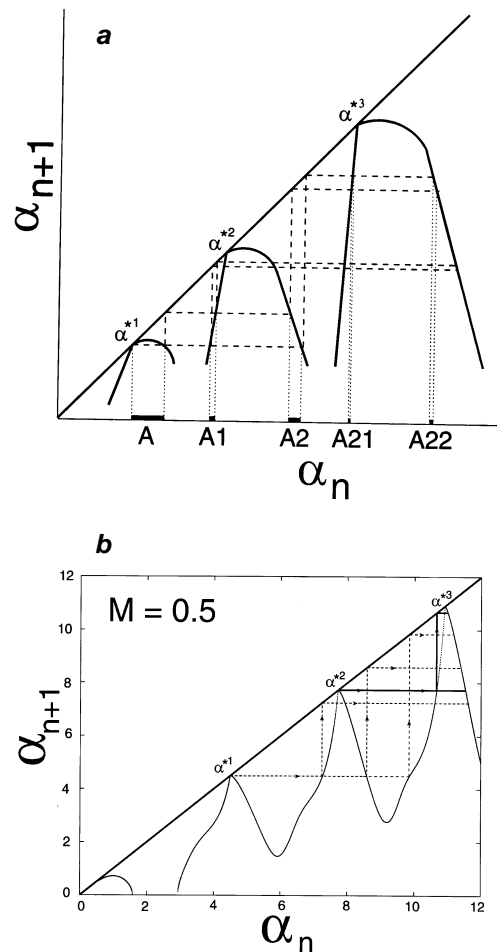


Figure 9. *a*, Basin of attraction for the fixed point \mathbf{a}^{*1} ; *b*, Initial conditions whose iterates converge to the fixed points $\mathbf{a}^{*1} = 4.4934$ and $\mathbf{a}^{*2} = 7.7252$.

Extended basin of attraction

In Figure 10, the basin of attraction is plotted for a particular M . We can plot the basin of attraction for a range of values of M . The extended basin of attraction is the set of all points in the $\mathbf{a} - M$ space which lead to incessant hopping, i.e. a set of all initial conditions that converge to a fixed point. The extended basin of attraction is shown in Figure 11 *a*. The inset in Figure 11 *a* is shown in detail in Figure 11 *b*. The basin of attraction has a structure which looks similar at finer scales. This means that if one zooms the inset in Figure 11 *b*, it would look similar to the basin in Figure 11 *b*.

Now, we try to explain a few features of the basin of attraction shown in Figure 11 *a*. Inspecting closely, we see the birth of a loop between the fixed points \mathbf{a}^{*2} ($= 7.7252$) and \mathbf{a}^{*3} ($= 10.9041$) at $M = 0.324$. We can see a similar loop occurring at $M = 0.17$ and $M = 0.116$. The reason for the occurrence of these loops is evident from Figure 12 *a* and *b*. If we use the staircase construction in reverse, then we realize that the map between the fixed points \mathbf{a}^{*2} and \mathbf{a}^{*3} becomes tangent to the straight line $\mathbf{a}_{n+1} = 4.493$ for $M = 0.324$ (see Figure 12 *a*). This means that if the starting point is the point of tangency, then its orbit would converge to the fixed point in a single iterate. For higher values of M , the map intersects the line at two points. Since the variation of M is continuous in the extended basin of attraction, this manifests as the occurrence of the loop in the extended basin of attraction at $M = 0.324$. For $M = 0.17$, the portion of the map between \mathbf{a}^{*2} and \mathbf{a}^{*3} becomes tangent to the straight line when we backtrack a second time (see Figure 12 *b*). This means that if the initial point is the point of tangency, its orbit would converge to the fixed point $\mathbf{a}_{n+1} = 4.493$ in two iterations. As the value of M is increased, the map inter-

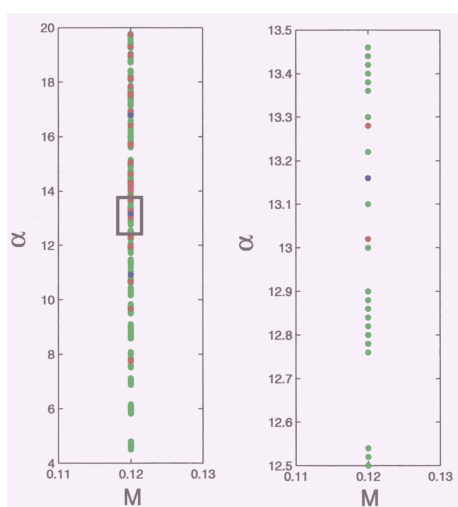


Figure 10. Basins of attraction due to different fixed points for $M = 0.12$. The inset in the figure on the left is shown in detail on the right.

sects the straight line at two points and this appears as the loop in the extended basin of attraction. For $M = 0.116$, the portion of the map between \mathbf{a}^{*2} and \mathbf{a}^{*3} becomes tangent to the straight horizontal line when we backtrack a third time.

Conclusions

We have studied a simple, passive spring-mass model which mimics hopping. The inelastic collisions with the rigid ground are the only mode of energy dissipation. The dynamics of the hopper consists of distinct phases, namely the take-off or the in-flight phase, the impact or the landing phase, and the phase immediately after the landing. The non-dimensional equations of motion are solved to get the initial non-dimensional velocity \mathbf{a} of the upper mass at take-off that leads to lossless collisions. The solutions are obtained by solving a trigonometric equation. The solutions are infinite in number and are a measure of the energy of the hopper at take-off. We construct a one-dimensional map, the map parameter being \mathbf{a} . The map is a recursive operation which takes an initial value of \mathbf{a} at take-off and gives the value of \mathbf{a} at the next gradual take-

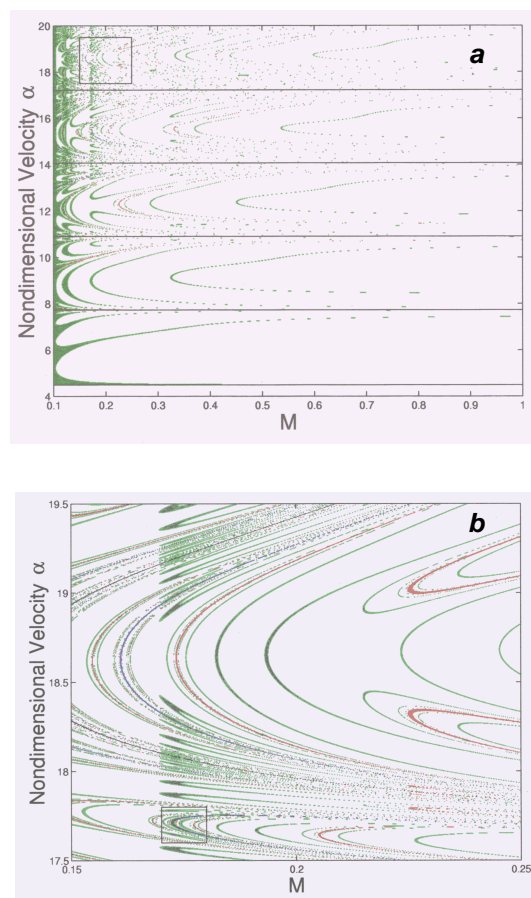


Figure 11. *a*, Extended basin of attraction; *b* The inset in (*a*) is shown in detail.

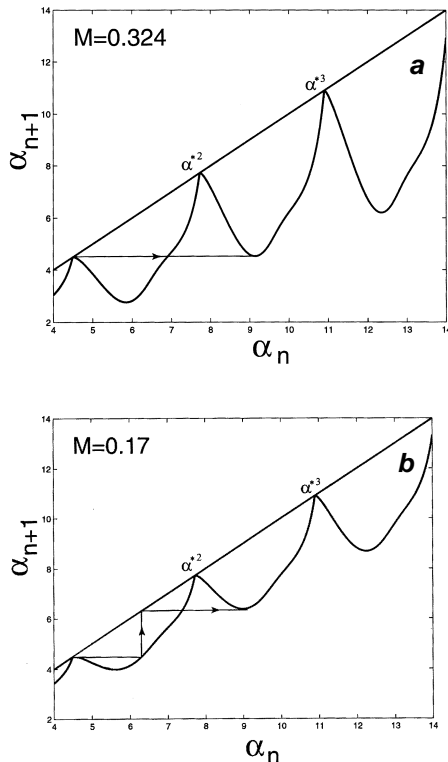


Figure 12. *a*, One-dimensional map for $M = 0.324$; *b* One dimensional map for $M = 0.17$.

off. We take a range of initial values of α and plot the one-dimensional map by obtaining the corresponding values of α at the next gradual take-off. The solutions that give lossless collisions are the fixed points of the map. The fixed points exhibit one-way stability, a feature that has been observed, to the best of our knowledge, for the first time in a mechanical system. We define the basin of attraction of the hopper and show that the basin of attraction is nested. We also construct the extended basin of attraction, which considers the effect of the system para-

meter M , the mass ratio, on the dynamics of the hopper. The extended basin of attraction has a complex structure and appears self-similar at finer scales. We explain a few prominent features of the extended basin of attraction through the study of the one-dimensional map.

1. Strogatz, S. H., *Nonlinear Dynamics and Chaos: With Applications to Physics, Biology, Chemistry and Engineering*, Addison-Wesley, 1994.
2. Holmes, P., *J. Sound Vib.*, 1982, **84**, 173–189.
3. Shaw, S. W. and Rand, R. H., *Int. J. Non-Linear Mech.*, 1989, **24**, 41–56.
4. Thompson, J. M. T. and Ghaffari, R., *Phys. Lett. A*, 1982, **91**, 5–8
5. Thompson, J. M. T. and Ghaffari, R., *Phys. Rev. A*, 1983 **27**, 1741–1743.
6. Bernard Brogliato, *Nonsmooth Impact Mechanics: Models, Dynamics and Control*, Springer, London, 1996.
7. Ivanov, A. P., *J. Sound Vib.*, 1994, **178**, 361–378.
8. Ivanov, A. P., *Chaos, Solitons Fractals*, 1996, **7**, 1615–1634.
9. M'Closkey, R. T. and Burdick, J. W., *Int. J. Robotics Res.*, 1993, **12**, 197–218.
10. Vakakis, A. F. and Burdick, J. W., *Int. J. Robotics Res.*, 1991, **10**, 606–618.
11. McGeer, T., *Int. J. Robotics Res.*, 1990, **9**, 62–82.
12. Coleman, M., Ph D dissertation, Cornell University, 1998.
13. Garcia, M., Ruina, A. and Chatterjee, A., International Conference on Robotics and Automation, 1997.
14. Garcia, M., Chatterjee, A. and Ruina, A., *ASME J. Biomech. Eng.*, 1998, **120**, 281–288.
15. Chatterjee, A., (pers. commun.)
16. Chatterjee, A., Pratap, R., Reddy, C. K. and Ruina, A., *Phys. Rev. Lett.*, (paper submitted).
17. Devaney, R., *An Introduction to Chaotic Dynamical Systems*, Addison-Wesley, New York, 1987.
18. Hale, J. and Kocak, H., *Dynamics and Bifurcations*, Springer-Verlag, New York, 1991.

ACKNOWLEDGEMENTS. This work has been supported by the Department of Science and Technology, Government of India through the grant no. III. 5(200)/99-ET. We thank Prof. Andy Ruina and Prof. Anindya Chatterjee for introducing them to this problem and for their invaluable suggestions at various stages.

Received 20 April 2000; revised accepted 13 July 2000